Morphology of Organic/Inorganic Aerosol with Varying Seed Particle Water Content

Emma C. Tackman¹, Devon N. Higgins², Murray V. Johnston², Miriam Arak Freedman^{1,3,*}

Abstract

The morphology of mixed organic/inorganic particles can strongly influence the physicochemical properties of aerosols but remains relatively less examined in particle formation studies. The morphologies of inorganic seed particles grown with either α -pinene or limonene secondary organic aerosol (SOA) generated in a flow tube reactor were found to depend on initial seed particle water content. Effloresced and deliquesced ammonium sulfate seed particles were generated at low relative humidity (<15% RH, dry) and high relative humidity (~60% RH, wet) and were also coated with secondary organic material under low growth and high growth conditions. Particles were dried and analyzed using SMPS and TEM for diameter and substrateinduced diameter changes and for the prevalence of phase separation for organic-coated particles. Effloresced inorganic seed particle diameters generally increased after impaction, whereas deliquesced inorganic seed particles had smaller differences in diameter, although they appeared morphologically similar to the effloresced seed particles. Differences in the changes to diameter for deliquesced seed particles suggest crystal restructuring with RH cycling. SOA-coated particles showed negative diameter changes for low organic growth, although wet-seeded organic particles changed by larger magnitudes compared to dry-seeded organic particles. High organic growth gave wide ranging diameter percent differences for both dry- and wet-seeded samples. Wet-seeded particles with organic coatings occasionally showed a textured morphology unseen in the coated

¹Department of Chemistry, The Pennsylvania State University, University Park, PA 16802, USA

²Department of Chemistry and Biochemistry, University of Delaware, Newark, DE 19716, USA

³Department of Meteorology and Atmospheric Science, The Pennsylvania State University, University Park, PA 16802, USA

^{*}To whom all correspondence should be addressed: maf43@psu.edu, 814-867-4267

particles with dry seeds. Using a flow tube reactor with a combination of spectrometry and microscopy techniques allows for insights into the dependence of aerosol particle morphology on formation parameters for two seed conditions and two secondary organic precursors.

Keywords: transmission electron microscopy, scanning mobility particle size spectrometry, secondary organic aerosol, Aitken mode, particle growth, flow tube reactor, liquid-liquid phase separation, aerosol phase transitions

1. Introduction

Aerosol particles are found throughout the atmosphere and are known to influence the global climate as well as human health, yet their specific effects are not fully understood. Organic material is a substantial and diverse component of atmospheric aerosol particles, representing between 20% and 90% of all particles by mass, and the pathways of formation and inclusion of organic compounds into aerosol particles is of continued interest.^{1,2} Mixed secondary organic/inorganic laboratory particles are a well-studied proxy system for environmental aerosol particles.^{3–5} Secondary organic material is commonly generated in a laboratory environment from the oxidation of atmospherically relevant monoterpenes, including α -pinene and limonene. α -Pinene is emitted from forest vegetation and is the most abundant of the monoterpenes.^{6–8} Limonene is another highly reactive monoterpene that may have a significant presence in indoor environments due to its inclusion in common household cleaners or other scented products. 9-11 The low volatility products of monoterpene oxidation can nucleate new particles, condense onto preexisting seed particles, or participate in reactive uptake into the particle phase, all of which result in the formation of secondary organic aerosol (SOA).¹² Ammonium sulfate, which is a common inorganic component in continental aerosol, is often used as laboratory seed particle material. Laboratory particles of mixed composition can be used to model aerosol systems that exist in the atmosphere and are frequently used to study aerosol particles under controlled conditions. These proxy aerosol particles allow for the systematic examination of the influence of particle-level formation parameters on the final physicochemical characteristics of more complex particles.¹³

The liquid water content, and, by extension, the phase state, of the inorganic seed particle at the time of coating with organic material has been shown to influence the physical and chemical properties of the resulting organic/inorganic mixed particles. 14-22 Several studies demonstrate the dependence of the terpene secondary organic chemical products of either reactive uptake or particle phase reactions on the liquid water content of the seed particle. 14-16,18-22 At high relative humidities above the deliquescence point of the inorganic salt, seed particles exist as liquid droplets and this aqueous phase is able to support chemical reactions like oxidation and oligomerization. 14,15 Higgins et al. saw a substantial increase in the conversion of α-pinene precursor to secondary organic material on deliquesced seeds compared with effloresced seeds due to reactions in the aqueous phase. 16 Song et al. reported that light absorbing products from acidcatalyzed oligomerization reactions were observed for SOA formation on acidic seeds under dry conditions, but disappeared at moderate relative humidities.¹⁷ This change was likely driven by high acidity conditions at low relative humidities, which was also seen by Nestorowicz et al. who described greater isoprene SOA yields on dry acidic seeds but minimal enhancement above 44% RH. 18 Seed particles at a high liquid water content have been shown to promote the partitioning of hydrophilic gas-phase species and reactive uptake of water-soluble compounds, enriching these species during the formation of α -pinene secondary organic coatings on deliquesced seeds. ^{14,19} A similar effect was seen for toluene SOA.^{20,21} Further, Huang et al. observed an enhancement of limonene SOA formation in the presence of a particle air-water interface over dry particles due to uptake of surface active volatile organic compounds, with greater enhancements at higher particle water volume fractions.²² Overall, volatile species are able to diffuse into deliquesced inorganic seed particles more easily than effloresced ones and the yield and chemical identities of the products of heterogeneous and particle phase reactions are altered at elevated relative humidities due in part to the increased accessible aqueous volume.^{14,16,18,20}

When mixed, organic and inorganic components within an aerosol particle can assume a variety of morphologies including phase separated or homogeneous configurations depending on the chemical components and local relative humidity.²³ Morphology can dramatically impact chemical and physical properties of aerosol particles. When particles are phase separated and form a core-shell morphology, the outer organic shell is known to limit particle reactivity through reduced diffusion of gaseous species into the particle.^{24–27} This inhibition is especially true at low relative humidities when organic phases can be glassy.^{28,29} Well-mixed particles also show different optical properties from phase separated particles of the same composition.^{30–33} Organic species enriched at the surface of a particle reduce its surface tension, leading to higher cloud condensation nuclei activity.³⁴ Most studies of the relative humidity-dependent formation of SOA examine chemical composition, usually with mass spectrometry.^{4,14,18–20,32,35,36} The physical morphology of SOA particles is a crucial determining factor for aerosol properties and reactivity, yet fewer investigations examine this aspect of particle formation.^{37,38}

Here, we use transmission electron microscopy (TEM) and scanning mobility particle size spectrometry (SMPS) to assess the influence of inorganic seed particle water content on the morphology and surface interactions of both inorganic ammonium sulfate seeds and mixed α -pinene or limonene secondary organic/inorganic aerosol particles. Two classes of inorganic seed particles, deliquesced (wet, ~60% RH) and effloresced (dry, <15% RH), are assessed using SMPS

and TEM. The wet seeds are deliquesced under supersaturated conditions and then equilibrated at \sim 60% RH, forming metastable aqueous nanodroplets with respect to ammonium sulfate, whereas the dry particles are maintained below 15% RH. Both classes of seeds are sent into a flow tube reactor where they are coated in freshly generated secondary organic material and analyzed for size and morphology. Limonene organic and wet particle measurements are compared to results from our previous study of α -pinene secondary organic material on dry particles. Importantly, water content classifications ("wet" and "dry") apply to the phase state of the particles within the flow tube reactor, and particles of all types are dried to <15% RH before collection to prevent coalescence and splatter upon impaction. "Seeds" refer to bare inorganic particles while "seeded particles" refer to the mixed organic/inorganic particles, usually with an indication of the seed phase state at the time of organic coating. The particles studied here are in the Aitken mode, which is the dominant atmospheric mode by number concentration, 40 and the two phase state extremes are used to represent contrasting atmospherically relevant conditions.

2. Methods

Detailed descriptions of the aerosol particle generation methods and analysis used here have been reported in previous studies (generation: Higgins et al., 2022 and analysis: Tackman et al., 2023). 16,39 In brief, samples of bare seed particles and α -pinene or limonene secondary organic coated particles were produced at the University of Delaware using a flow tube reactor and shipped on dry ice to the Pennsylvania State University for analysis.

To generate deliquesced seed particles, atomized ammonium sulfate (99.9995%, Sigma-Aldrich Co.) particles were dried and size selected using a differential mobility analyzer (DMA, SI 3085). This flow was then humidified in a condensational growth chamber (CGC, custom

device from Aerosol Dynamics Inc.) where the particles were exposed to temperature-controlled regions of supersaturated water vapor to produce deliquesced droplets. The humidified particles were then directed into the flow tube reactor with ozone and water vapor to maintain the relative humidity around 60%. For organic growth experiments, a flow of α -pinene (98%, Sigma-Aldrich Co.) or limonene (97%, Acros Organics) was also added to the flow tube to react with ozone and form secondary organic material which condensed onto the seed particles. Different levels of organic growth were achieved using constant ozone concentrations, between ~275-350 ppbv O₃, and varying concentrations of secondary organic precursor. For α -pinene, concentrations ranged from 5-10 ppbv for low growth experiments and 10-100 ppbv for high growth experiments. For limonene, ranges were 5-35 ppbv for low growth experiments and 10-200 ppbv for high growth. Low growth conditions yielded thin organic coatings with a total thickness below a certain threshold value as measured by the change in mobility diameter, while high growth conditions yielded thicker coatings with a total thickness greater than the threshold. Threshold values were 11 nm for α -pinene and 6 nm for limonene.

Populations of effloresced seeds and effloresced seeds with organic coatings were generated in the same way as deliquesced samples, but without the condensational growth chamber and final diffusion dryer, which caused the effloresced samples to remain below 15% RH for the duration of the experiment. A schematic of the flow tube configuration and the particle flows used here can be found in the Supplementary Information (Figure S1).

Finally, in order to provide a stable environment for SMPS analysis and to prevent particle splatter upon impaction, the seeds or coated particles exiting the flow tube were passed through a diffusion dryer to rapidly decrease the relative humidity to <15%. In addition to SMPS measurements, particles were collected onto TEM grids made of continuous carbon film at

standard thickness over a 200-mesh copper support (Electron Microscopy Science) using a nanometer aerosol sampler (NAS, TSI 3089). It is of particular importance that low relative humidity was maintained around samples between the times of collection and imaging to prevent changes to morphology caused by freezing and thawing of moisture within the particles. Samples of deposited particles were packed in desiccant and frozen immediately after generation at the University of Delaware. Batches of prepared samples were shipped overnight when possible from the University of Delaware to the Pennsylvania State University on dry ice to prevent water vapor from accumulating during transfer. After arrival at the Pennsylvania State University, sample-laden grids were placed in a desiccator to thaw and were analyzed promptly (typically within one week). Control experiments performed and published previously show that particles are stable in storage under these conditions.

Additional effloresced seed samples were generated at the Pennsylvania State University to ensure that the freezing and shipping process did not influence the samples. For these samples, a 0.1 wt% ammonium sulfate (ACS Grade, Millipore) solution was atomized (TSI 3076) and the resulting particles were rapidly dried to <10% RH in a diffusion dryer, size selected using an electrostatic classifier (TSI 3080) and a DMA (TSI 3081), and deposited onto a TEM substrate using a cascade impactor (8-stage mini-MOUDI, Model 135, MSP Corp.). As with the samples made at the University of Delaware, the substrates were a standard carbon/copper grid (Electron Microscopy Science) and samples were analyzed within one week of generation. Nominal median electrical mobility diameters are reported for these samples.

TEM studies were performed using a Talos F200C (FEI) with the cryo box engaged for all samples. Samples were cooled to cryogenic temperatures using liquid nitrogen in single tilt cryoholders (Gatan) and the cryo box prevented ice accumulation on the sample. Cryogenic conditions

were maintained around the grid during analysis to reduce beam damage to the particles. Particle size analysis was performed in ImageJ (NIH) by manually selecting particle and core perimeters for area-equivalent diameter calculations. Resolution for TEM depends on the magnification used, but typical pixel values for this study are 0.32 nm/pixel or 0.4 nm/pixel. For all experiments, no unexpected or unusually high safety hazards were encountered.

3. Results

Effloresced and deliquesced ammonium sulfate seeds and proxy organic aerosol particle sizes were characterized using SMPS and TEM and particle morphologies using TEM. The morphological features assessed in this study were electrical mobility diameter (D_m, SMPS) for suspended particles, projected area-equivalent diameter (D_{pa}, TEM) for impacted particles, particle shape, and phase separation. Particle-surface interactions were also investigated through changes to the median diameter of the particle populations before and after collection onto a substrate. These changes are reported as a percent difference, defined in Equation 1:

(1)
$$Percent Difference = \left(\frac{D_{pa} - D_{m}}{D_{m}}\right) \times 100$$

or in other words, the difference between a particle's diameter after impaction compared to its suspended diameter. Expressly, for a particle population with an increased median diameter after substrate deposition, D_{pa} will be greater than D_{m} and the percent difference will be positive. It is worth emphasizing again that all populations of wet particles, both seeds and coated particles, passed through a diffusion dryer after exiting the flow tube, and thus all diameters reported for wet samples are for particles that have undergone this final drying step. As a visual guide, graphics illustrating the expected morphology and water content for each type of particle at each stage of generation can be found in Figures S2 and S3 in the supplement. Specifically, wet particles

experienced an additional deliquescence-efflorescence cycle while dry particles remained effloresced after the size-selection step for the entirety of the experiment. For a similar experimental setup, Faust et al. found that α -pinene secondary organic material on deliquesced seeds did not evaporate with statistical significance after passing through a diffusion dryer after coating.¹⁴ So, in the studies reported here, we expect that most of the water is removed before SMPS analysis and sample collection with minimal effect on the organic content.

3.1 Wet and Dry Seed Particles

The D_m of suspended deliquesced and effloresced ammonium sulfate seed populations were measured using SMPS. The same populations of particles were deposited onto a substrate and analyzed using TEM for morphology and D_{pa}. Figure 1 shows typical D_m and D_{pa} distributions for the size selected deliquesced and effloresced seeds as well as a representative image of a particle of each type. Generally, both deliquesced and effloresced particles had similarly round shapes and an even contrast with the background as shown in Figures 1b and 1d. However, the two types of seeds showed dissimilar behaviors after deposition onto a substrate, in terms of the signs and magnitudes of their percent changes in diameter. Table 1 enumerates the median D_m and D_{pa} for each population of wet and dry seed particles and their respective percent changes. After impaction, dry ammonium sulfate seeds increased in diameter by between +0% and +30% of their suspended diameters while wet ammonium sulfate seed droplets changed by -6% to +4% of their suspended diameters. For dry seed particles these ranges represent numerical diameter increases of +0.1 nm to +18.8 nm, and for wet particles these changes demonstrate diameter changes from -4.0 nm to +1.4 nm. These are the minimum and maximum values from calculating the difference between the Median (TEM) column and Median (SMPS) column for each sample in Table 1.

Figure S4 graphically depicts the D_{pa} vs. D_{m} relationship for wet and dry seeds where percent differences are shown as deviations from a one-to-one line.

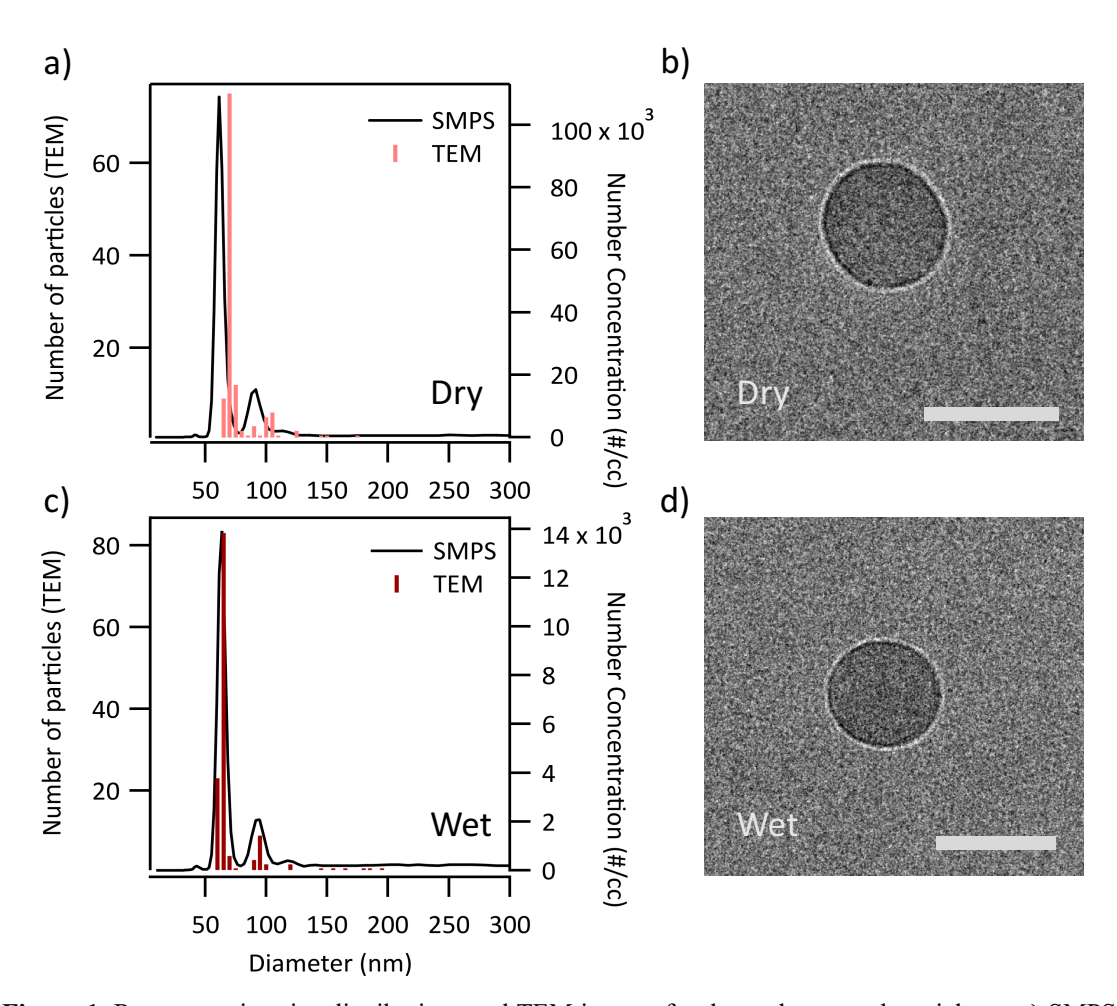


Figure 1. Representative size distributions and TEM images for dry and wet seed particles. **a,c)** SMPS size distributions (solid lines) show the number of suspended particles vs. D_m and the TEM size distributions (colored bars) show the number of deposited particles vs. D_{pa} for the same population of aerosol seed particles. **b,d)** TEM images of wet and dry seed particles show that both types of seeds have similar appearances with rounded shapes and even contrast. Scale bars 50 nm.

Table 1. Wet and Dry Ammonium Sulfate Seed Particles

Seed Type	Generation	n ^a	Median D _m (SMPS) ^b	Median D _{pa} (TEM) ^c	% difference ^d
	University of Delaware	53	39.9 nm	44.4 nm	+11%
		111	39.5 nm	40.1 nm	+1%
Dry*		55	39.5 nm	40.1 nm	+1%
Diy		185	40.1 nm	42.1 nm	+5%
		208	37.5 nm	48.9 nm	+30%
		127	41.6 nm	44.7 nm	+7%

		129	41.5 nm	44.3 nm	+7%
		10	61.3 nm	64.9 nm	+6%
		122	61.0 nm	65.4 nm	+7%
		185	61.1 nm	61.0 nm	0%
		111	64.0 nm	68.6 nm	+7%
		136	63.0 nm	77.3 nm	+23%
		120	62.7 nm	68.3 nm	+9%
	The	30	80 nm	85.6 nm	+7%
	Pennsylvania State	16	80 nm	87.7 nm	+10%
	University	105	100 nm	118.8 nm	+19%
		53	42.7 nm	42.2 nm	-1%
		129	42.7 nm	41.4 nm	-3%
		59	41.6 nm	40.2 nm	-3%
		133	42.6 nm	41.2 nm	-3%
	TT	113	43.7 nm	44.4 nm	+2%
Wet	University of Delaware	113	36.7 nm	38.2 nm	+4%
		115	66.9 nm	68.4 nm	+2%
		101	64.9 nm	61.0 nm	-6%
		134	65.5 nm	61.6 nm	-6%
		214	60.9 nm	60.1 nm	-1%
		227	60.3 nm	59.8 nm	-1%

^a number of particles analyzed per sample

3.2 Secondary Organic Growth of Wet and Dry Seeds

The morphologies of effloresced and deliquesced ammonium sulfate seeds grown by the formation of α -pinene and limonene secondary organic aerosol material generated under low and high organic growth regimes were assessed for dependence on the water content of the initial inorganic seed. α -Pinene results are shown in Figures 2 and 3 and limonene results are displayed in Figure 4 and 5. Figures 2 and 4 show typical D_m and D_{pa} size distributions for populations of particles with low secondary organic growth on deliquesced and effloresced ammonium sulfate seeds and a representative image of a phase separated particle for each seed type. Figures 3 and 5 show the same for high growth samples. All images in Figures 2-5 show a shell of organic material

b median particle mobility diameter (D,,,)

e median particle projected area diameter (D_{na})

^d percent difference between the median mobility diameter and median projected area diameter as defined by Equation 1

^{*}Results from Tackman et al., 202339

around an ammonium sulfate core with a visible phase boundary indicated by a white arrow. The percentage of particles from each sample showing phase separated and homogeneous morphologies along with the median core D_{pa} and shell thickness for phase separated particles as determined from TEM imaging are given in Tables 2 and 3. Also presented are the corresponding seed size and change in D_m from organic growth, or organic shell thickness, of the suspended particles as observed via SMPS. Finally, median D_m and D_{pa} for each population are given along with their corresponding percent differences.

3.2.1 α -Pinene

α-Pinene sample populations with low organic growth consistently showed decreases to median diameters after impaction with dry-seeded particles displaying negative percent differences by -6% to -9% of their initial diameters and low organic growth on wet seeds exhibiting slightly larger negative percent differences from -9% to -13%. These ranges in percent differences represent numerical diameter decreases of -2.9 nm to -5.9 nm for low growth on dry seeds, and -5.9 nm to -7.6 nm for low growth on wet seeds. These are the maximum and minimum values found from calculating the difference between the Median (TEM) column and Median (SMPS) column for each α-pinene sample in Table 2. For α-pinene high growth samples on both dry and wet seeds, a wide range of percent changes were observed. Between +48% and -36% differences in diameter were observed for α-pinene high growth on dry seeds and between -19% and -35% differences were seen for the same on wet seeds. These ranges in percent differences represent diameter changes of +33.0 nm to -31.3 nm for high growth on dry seeds, and diameter decreases between -12.1 nm and -28.1 nm for high growth on wet seeds. These are the maximum and minimum values found from calculating the difference between the Median (TEM) column

and Median (SMPS) column for each α -pinene sample in Table 3. Figure S5 graphically depicts the D_{pa} vs. D_m relationship for α -pinene secondary organic growth on wet and dry seeds where percent differences are shown as deviations from a one-to-one line. In all cases, α -pinene high organic growth on both wet and dry seeds showed size deviations of larger magnitude after substrate deposition than low growth samples.

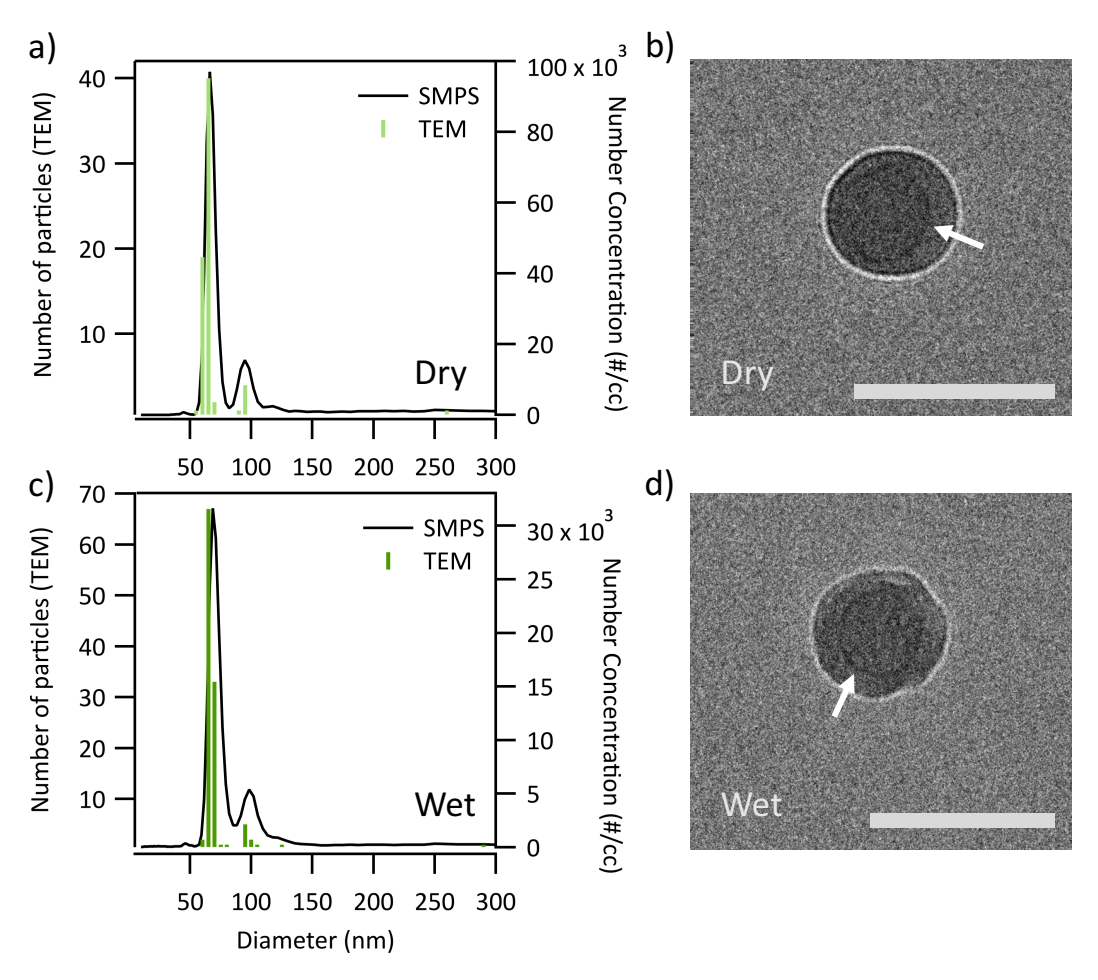


Figure 2. Representative size distributions and TEM images for α -pinene secondary organic low growth on dry and wet seed particles. **a,c**) SMPS size distributions (solid lines) show the number of suspended particles vs. D_m and the TEM size distributions (colored bars) show the number of deposited particles vs. D_{pa} for the same population of coated aerosol particles. **b,d**) TEM images of low α -pinene secondary organic growth on wet and dry seed particles displaying phase separation. Secondary organic coatings surround ammonium sulfate cores with visible phase boundaries indicated by a white arrow. The wet-seeded organic particle in panel D shows a textured morphology. Scale bars 100 nm.

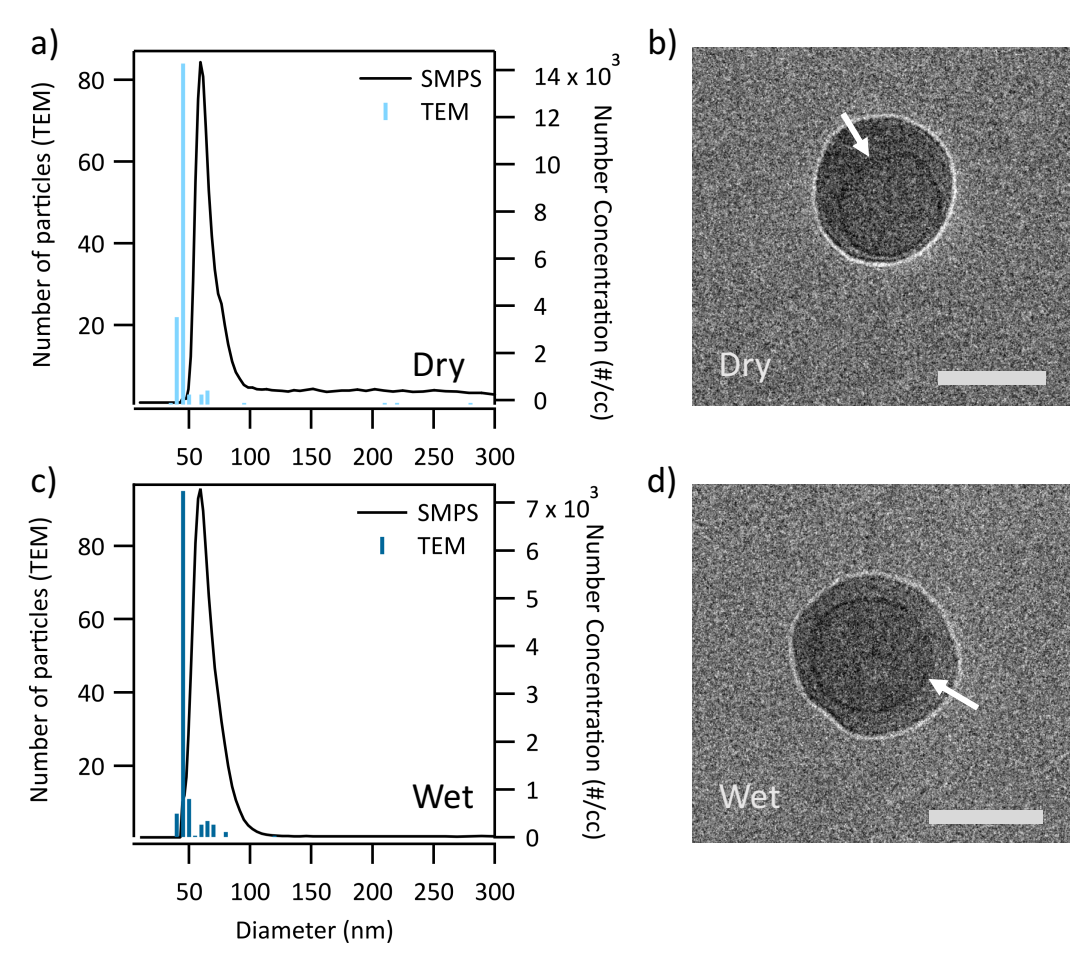


Figure 3. Representative size distributions and TEM images for α -pinene secondary organic high growth on dry and wet seed particles. **a,c)** SMPS size distributions (solid lines) show the number of suspended particles vs. D_m and the TEM size distributions (colored bars) show the number of deposited particles vs. D_{pa} for the same population of coated aerosol particles. Both wet and dry TEM distributions are at a significant negative offset from the corresponding SMPS distributions, indicating the negative percent differences observed for most of these populations. **b,d)** TEM images of high α -pinene organic growth on wet and dry seed particles displaying phase separation. Secondary organic coatings surround ammonium sulfate cores with visible phase boundaries indicated by a white arrow. The wet-seeded organic particle in panel D shows a mildly textured morphology. Scale bars 50 nm.

Table 2. Low Organic Growth on Wet and Dry Seed Particles

SOA Type ^{&}	Seed Type	n ^a	Median D _m (SMPS) ^b	Median D _{pa}		% phase separated ^e	% homogeneous f	Growth (SMPS) ^g	Growth (TEM) ^h	Seed Size (SMPS) ⁱ	Core Size (TEM)
		48	45.6 nm	42.6 nm	-7%	19%	77%	5.7 nm	10.0 nm	39.4 nm	37.4 nm
		98	45.6 nm	42.4 nm	−7%	51%	43%	5.7 nm	8.0 nm	39.4 nm	33.7 nm
	Drv*	127	47.1 nm	44.2 nm	-6%	47%	39%	4.0 nm	3.3 nm	43.1 nm	40.9 nm
α-Pinene	Dry	227	66.6 nm	61.1 nm	-8%	68%	27%	5.5 nm	13.7 nm	61.1 nm	48.1 nm
		68	68.0 nm	62.0 nm	-9%	43%	42%	5.2 nm	18.3 nm	62.8 nm	41.6 nm
		127	68.5 nm	63.0 nm	-8%	84%	11%	5.8 nm	14.5 nm	62.8 nm	49.7 nm
	Wet	74	47.8 nm	41.7 nm	-13%	95%	1%	4.3 nm	10.4 nm	44.0 nm	31 nm

		203	47.2 nm	41.4 nm	-12%	97%	2%	2.8 nm	9.2 nm	44.4 nm	32.5 nm
		51	77.9 nm	71.1 nm	-9%	14%	84%	10.3 nm	4.1 nm	67.7 nm	65.4 nm
		112	77.8 nm	71.1 nm	-9%	5%	92%	10.3 nm	3.8 nm	67.7 nm	69.1 nm
		114	71.3 nm	64.4 nm	-10%	3%	2%	6.1 nm	NA	65.2 nm	NA
		147	72.7 nm	65.1 nm	-10%	1%	2%	7.5 nm	NA	65.2 nm	NA
		130	40.6 nm	35.7 nm	-12%	95%	3%	4.5 nm	7.3 nm	36.1 nm	28.6 nm
		156	41.8 nm	36.5 nm	-13%	56%	44%	5.8 nm	3.7 nm	36.1 nm	32.5 nm
	Dry	179	37.8 nm	36.3 nm	-4%	89%	9%	2.2 nm	4.5 nm	37.8 nm	31.8 nm
Limonene		220	39.7 nm	39.2 nm	-1%	36%	64%	1.9 nm	2.7 nm	37.8 nm	36.7 nm
		178	40.2 nm	41.9 nm	+4%	10%	90%	2.4 nm	2.5 nm	37.8 nm	51.0 nm
	Wet	180	47.3 nm	43.3 nm	-8%	51%	49%	4.0 nm	4.2 nm	43.3 nm	37.9 nm
	******	209	48.9 nm	42.8 nm	-12%	64%	94%	5.6 nm	12.6 nm	43.3 nm	31.0 nm

^a number of particles analyzed per sample

Table 3. High Organic Growth on Wet and Dry Seed Particles

SOA Type ^{&}	Seed Type		Median D _m (SMPS) ^b	Median D _{pa} (TEM) ^c	% difference	% phase separated ^e	% homogeneous	Growth (SMPS) ^f	Growth (TEM) ^g	Seed Size (SMPS) ^h	Core Size (TEM)
		30	56.1 nm	41.7 nm	-26%	73%	14%	16.6 nm	8.4 nm	40.0 nm	33.6 nm
		114	71.2 nm	105.4 nm	+48%	41%	36%	30.3 nm	70.2 nm	40.9 nm	39.3 nm
		92	48.0 nm	42.5 nm	-11%	7%	91%	13.1 nm	5.7 nm	37.6 nm	32.0 nm
		121	64.4 nm	41.4 nm	-36%	92%	5%	22.2 nm	4.8 nm	42.2 nm	36.5 nm
	Dry [*]	155	62.9 nm	42.3 nm	-33%	88%	9%	20.7 nm	4.3 nm	42.2 nm	38.2 nm
		60	101.3 nm	77.1 nm	-24%	43%	45%	40.6 nm	5.5 nm	62.7 nm	105.4 nm
α-Pinene		147	103.2 nm	72.0 nm	-30%	65%	29%	40.6 nm	5.0 nm	62.7 nm	93.8 nm
		92	77.5 nm	62.8 nm	-19%	45%	54%	15.2 nm	25.3 nm	62.4 nm	37.0 nm
		174	77.9 nm	62.4 nm	-20%	80%	14%	15.5 nm	24.2 nm	62.4 nm	38.4 nm
		105	58.7 nm	46.6 nm	-21%	38%	52%	14.0 nm	3.8 nm	44.7 nm	49.2 nm
	Wet	59	84.0 nm	66.3 nm	-21%	88%	9%	17.1 nm	13.8 nm	66.9 nm	53.6 nm
	VV Ct	107	82.3 nm	66.4 nm	-19%	81%	5%	15.8 nm	31.0 nm	66.5 nm	35.6 nm
		37	85.8 nm	69.8 nm	-19%	78%	8%	21.1 nm	19.9 nm	64.6 nm	48.5 nm

 $^{^{\}rm b}$ median particle mobility diameter (${\rm D_{\rm m}}$)

 $^{^{}c}$ median particle projected area diameter (D_{pa})

 $^{^{\}rm d}$ percent difference between the median $D_{\rm m}$ and median $D_{\rm pa}$ as defined by Equation 1

e percent of particles displaying obvious phase separation

^t percent of particles displaying obvious homogeneous morphology

 $^{^{\}rm g}$ particle growth observed by SPMS defined by the difference in $D_{\rm m}$ before and after the coating process

^h particle growth observed by TEM defined by the difference between the D_{pa} of the full particle and the D_{pa} of the core phase, or else twice the shell thickness

median D_m of the seed particles before coating

 $^{^{}J}$ median D_{pa} of the core phase in the coated particle

[&]amp; All samples were generated at the University of Delaware

^{*}Results from Tackman et al., 2023³⁹

		130	60.9 nm	42.6 nm	-30%	83%	15%	18.5 nm	5.9 nm	42.9 nm	36.9 nm
		154	80.8 nm	52.7 nm	-35%	81%	1%	15.8 nm	19.0 nm	65.0 nm	33.9 nm
		74	54.0 nm	37.5 nm	-31%	92%	4%	16.1 nm	7.4 nm	37.9 nm	30.5 nm
	Dry	153	55.1 nm	37.8 nm	-31%	74%	24%	17.5 nm	5.2 nm	37.7 nm	32.7 nm
		189	47.7 nm	37.2 nm	-22%	82%	3%	9.9 nm	7.5 nm	37.9 nm	30.2 nm
		149	48.4 nm	36.9 nm	-24%	92%	6%	10.6 nm	7.2 nm	37.8 nm	30.0 nm
Limonene		212	66.4 nm	44.7 nm	-33%	45%	54%	21.7 nm	5.3 nm	44.6 nm	39.1 nm
	Wet	214	66.4 nm	44.6 nm	-33%	63%	37%	21.8 nm	5.9 nm	44.6 nm	39.0 nm
	Wet	106	69.2 nm	51.1 nm	-26%	3%	93%	24.1 nm	NA	45.1 nm	NA
		108	54.5 nm	38.1 nm	-30%	71%	27%	10.8 nm	6.35 nm	43.6 nm	32.17 nm
		161	52.5 nm	39.1 nm	-26%	61%	37%	8.87 nm	6.54 nm	43.6 nm	31.89 nm

Column descriptions found in notes below Table 2

3.2.2 Limonene

Samples with limonene secondary organic low growth exhibited variable changes in diameter after impaction. Limonene low growth populations with dry seeds showed a range of both positive and negative percent differences from -12% to +4%, which was the largest range in percent changes for any of the low growth samples for either SOA type. Populations with wet seeds ranged in percent change from -8% to -12%. These ranges in percent differences represent numerical diameter changes spanning -5.3 nm to +1.7 nm for low growth on dry seeds, and -4.0 nm to -6.1 nm for low growth on wet seeds. These are the maximum and minimum values found from calculating the difference between the Median (TEM) column and Median (SMPS) column for each limonene sample in Table 2. Narrower ranges in percent changes were observed for limonene high growth samples on both dry and wet seeds when compared to α -pinene high growth samples. Between -22% and -31% differences in diameter were seen for thick coatings of limonene growth on dry seeds and between -24% and -33% differences were seen for the same on wet seeds. These ranges in negative percent differences represent diameter changes of -10.5 nm to -17.3 nm for high growth on dry seeds, and diameter decreases between -11.5 nm and -11.5

21.8 nm for high growth on wet seeds. These are the maximum and minimum values found from calculating the difference between the Median (TEM) column and Median (SMPS) column for each limonene sample in Table 3. Figure S5 also graphically depicts the D_{pa} vs. D_{m} relationship for limonene secondary organic growth on wet and dry seeds.

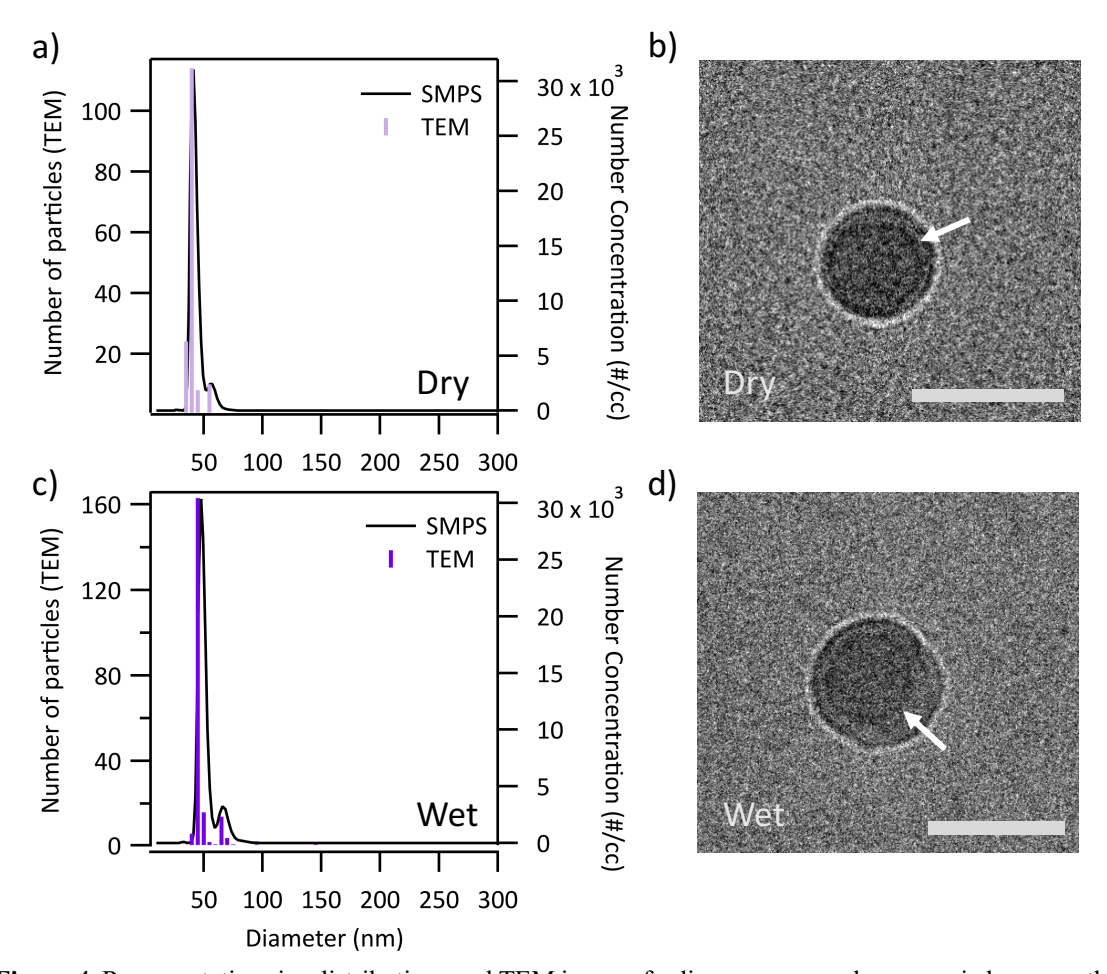


Figure 4. Representative size distributions and TEM images for limonene secondary organic low growth on dry and wet seed particles. **a,c)** SMPS size distributions (solid lines) show the number of suspended particles vs. D_m and the TEM size distributions (colored bars) show the number of deposited particle vs. D_{pa} for the same population of coated aerosol particles. Size distributions for both wet- and dry-seeded populations are as a slight negative offset, indicating the small negative percent differences typical for these populations. **b,d)** TEM images of low limonene secondary organic growth on wet and dry seed particles displaying phase separation. Secondary organic coatings surround ammonium sulfate cores with visible phase boundaries indicated by a white arrow. The wet-seeded organic particle in panel D shows a mildly textured morphology. Scale bars 50 nm.

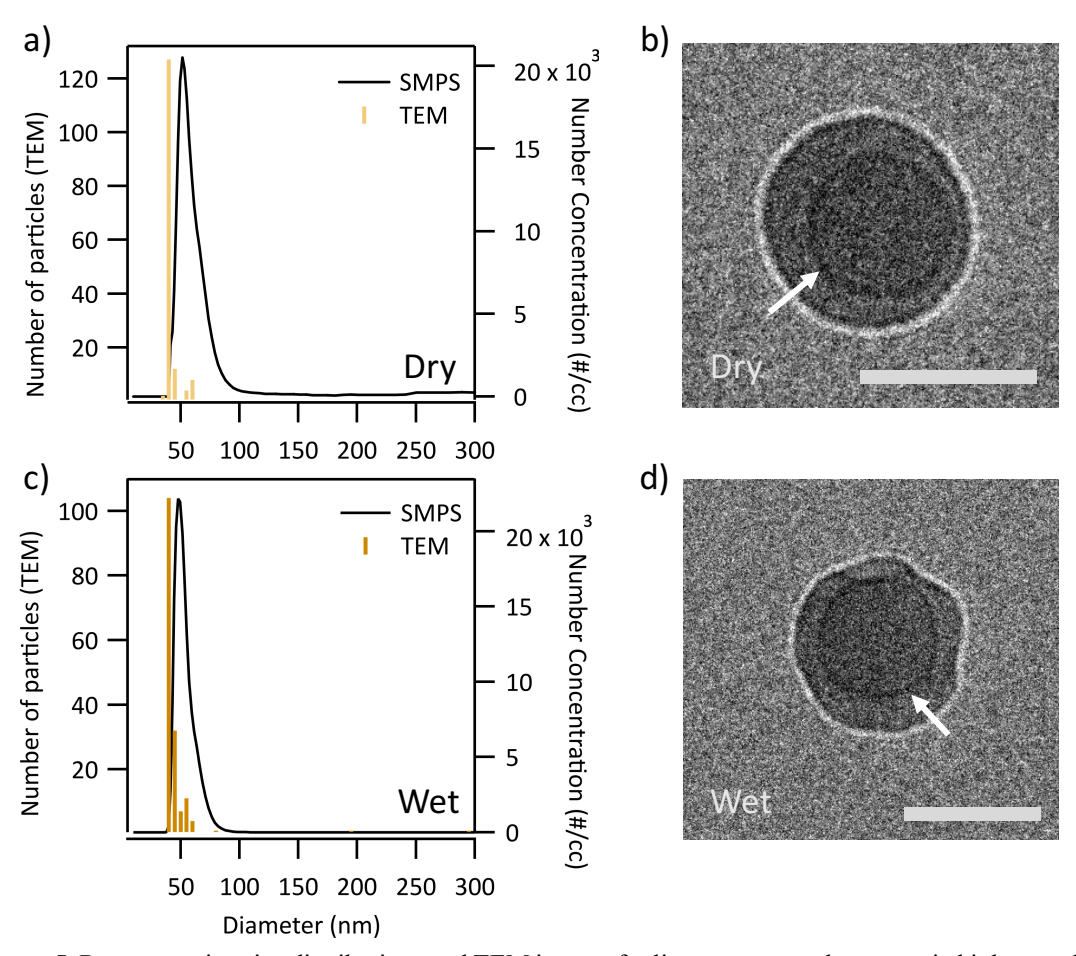


Figure 5. Representative size distributions and TEM images for limonene secondary organic high growth on dry and wet seed particles. \mathbf{a} , \mathbf{c}) SMPS size distributions (solid lines) show the number of suspended particles vs. D_m and the TEM size distributions (colored bars) show the number of deposited particles vs. D_{pa} for the same population of coated aerosol particles. Both wet and dry TEM distributions are at a significant negative offset from the corresponding SMPS distributions, indicating smaller diameters for these particles after deposition. \mathbf{b} , \mathbf{d}) TEM images of high limonene secondary organic growth on wet and dry seed particles displaying phase separation. Secondary organic coatings surround ammonium sulfate cores with visible phase boundaries indicated by a white arrow. The wet-seeded organic particle in panel D shows a textured morphology. Scale bars 50 nm.

4. Discussion

4.1 Wet and Dry Seed Particles

A difference between suspended and impacted median diameters was observed for all seed particle populations at each water content and the magnitudes and signs of these changes are expressed as percent differences in Table 1 and visually in Figure S4. Changes in seed diameter might be observed as a result of changes in particle volume or else impaction and spreading.

Presumably, inorganic seed particles with positive percent changes can be said to have spread along the substrate surface. Lee et al. saw an approximately 13% increase in particle width after impaction onto a substrate for a dry sodium chloride particle. For this experiment, it is unlikely that particles increased in volume in desiccated storage and under vacuum conditions within a TEM, so any positive changes in diameter with conserved particle volume are inferred to be a consequence of horizontal particle deformation upon impaction. Spreading, characterized by a positive percent change to median diameter, is observed in all dry seed particle samples, as well as several wet seed particle samples.

Either physical restructuring or loss of residual water likely accounts for the negative changes in diameter for some wet particle samples. Higgins et al. previously examined dry and wet ammonium sulfate seed particles at 60% RH in the same flow tube apparatus used for this study. 16 This relative humidity falls between the efflorescence and deliquescence relative humidities of ammonium sulfate, enabling the study of ammonium sulfate seeds with different water content under equivalent conditions. Dry seed particles did not change in diameter when passed through the apparatus, even at this elevated relative humidity. Wet particles, or in other words, particles that underwent an additional deliquescence-efflorescence cycle, had slightly larger mobility diameters after the final drying step by an average of 0.9 nm. This minor increase in diameter could imply some small amount of water was retained after exiting the final diffusion dryer, which could result in the small negative percent changes in diameter after impaction should this water be lost during storage or analysis. Restructuring could also account for some amount of the difference between D_m and D_{pa} as shape is important for SMPS analysis. The further a particle's shape deviates from a sphere, the larger the difference between D_m and D_{pa} will be for that same particle. If microstructural rearrangements introduce physical irregularities, particles' circularities

may decrease causing the small differences seen for some of the wet seed samples in Table 1 as well. The SI has further discussion of particle circularity.

The magnitudes of the changes in diameter for the wet seeds were lower than those for dry seeds, meaning that diameters remained more stable through the impaction process for wet particles. This effect can be observed in the diameter size distributions for wet and dry particles. In Figure 1a, the D_{pa} histogram derived from TEM measurements for dry particles is at a significant positive offset from the D_m histogram from SMPS measurements, denoting the spreading for all dry particles after impaction. The two histograms for the wet particles in Figure 1c, however, display very little offset, demonstrating the small magnitudes of the changes to diameter for wet particles and showing that the particles remained a similar size before and after impaction. The smaller changes in diameter for wet particles can also be seen in Figure S4 where the wet population median diameters tend to be much closer to the one-to-one line than the dry particle median diameters.

The smaller magnitude of the differences in size for wet particles are attributed to the increased density of the wet seeds due to microstructural rearrangements as they go through an additional deliquescence-efflorescence cycle in the flow tube apparatus. Many examples of such restructuring can be found in the literature. Beaver et al. recognized void spaces in ammonium sulfate aerosol particles where the density of the ammonium sulfate crystals decreased after atomization and transformation into dry particles.⁴³ Further, Hsiao et al. found that both atomized sodium chloride and ammonium sulfate nanoparticles increased in density and approached the bulk densities of their respective bulk materials upon gradual rehydration at relative humidities above 60%.⁴⁴ In agreement, Mikhailov et al. humidified ammonium sulfate particles generated through nebulization and drying and observed an initial ~3% *decrease* in mobility diameter upon increasing

relative humidity from 20% RH to 50% RH (as well as a 7% decrease in mobility diameter for organic oxalic acid particles humidified to 40%).⁴⁵ This decrease was associated with the compaction of irregularities within the initial salt crystal structure with hydration and before hygroscopic growth above 50% RH. A 1-2% decrease in D_m for ammonium sulfate particles was also identified by Biskos et al. under comparable conditions, noting somewhat nonspherical particle shapes at very low relative humidities that restructure to compact spheres upon humidification from 5% RH to 30% RH.⁴⁶ Köllensperger et al. too saw a decrease in ammonium sulfate particle volume as a result of partial dissolution and restructuring after exposure to high relative humidity.⁴⁷ Krämer et al. saw a similar phenomenon for sodium chloride, where nebulized and dried salt particles decreased in mobility diameter up to nearly 50% upon initial hydration between ~1% RH and 30% RH, again corresponding to particle compaction as a result of microstructural rearrangements.⁴⁸ These studies all reflect a decrease in crystal irregularities and a subsequent increase in density after rehumidification.⁴⁹

The smaller changes in diameter after impaction for wet seed particles relative to dry seeds seen in the experiments presented here may be a consequence of the changes to their microstructure from deliquescence-efflorescence cycling. Although both wet and dry ammonium sulfate seed particles appeared to be fairly round and lacked the irregular shapes expected by Mikhailov et al. and Biskos et al. when imaged using TEM, it is reasonable to assume that imperfections like voids or grain boundaries within the salt crystal structures were present upon initial atomization and drying. Voids can clearly contribute to overall particle volume and polycrystallinity decreases density through slightly increased atomic spacings at grain boundaries.⁴⁹ When the wet seed particles are humidified in the condensational growth chamber and subsequently dried for a second time, their volume void fraction or polycrystallinity decreases and density increases. Dry particles,

on the other hand, retain these crystal imperfections and have a lower final density than the wet particles. At the macro scale, higher density materials are generally more resistant to inelastic deformations due to higher Young's moduli. Onversely, for nanocrystalline materials, the Hall-Petch effect shows that grain boundaries can significantly increase yield strength, which describes the ability for a material to resist inelastic deformation. However, when crystal grains are sufficiently small, density and deformation resistance are again positively correlated, called the inverse Hall-Petch effect. The grain diameter at which the Hall-Petch effect breaks down depends on the material, but is usually a few 10s of nanometers. We suggest that grains in any polycrystalline structures within our particles are few or small enough to fall within the inverse Hall-Petch regime. Therefore, when dry particles are impacted, the lower density particles spread on the substrate to a greater degree, permanently deforming away from their suspended diameters. The higher density wet particles spread less and stay at a size closer to their suspended diameters than dry particles.

4.2 Secondary Organic Growth of Wet and Dry Seeds

4.2.1 Size analysis

While dry seeds with secondary organic coatings showed both positive and negative percent differences in diameter after deposition, all coated particles with wet seeds had negative percent changes. This point of contrast can be observed in Figure S5 where some median diameters for populations of organic coatings on dry seeds fall above the one-to-one line while median diameters for samples with wet seeds exclusively appear below the one-to-one line. Percent changes to median diameter after substrate collection can be explained through volume changes or the interactions between the surface and the particle. As with the seed particles, coated particles with positive percent changes after impaction have increased in diameter due to spreading. With

the addition of organic coatings, spreading could also be a result of flow of the viscous organic phase along the substrate. However, secondary organic particles with negative percent differences, those smaller after substrate deposition, have also been observed to spread on a surface.³⁹ For particles to both spread and also display negative percent changes in diameter after impaction, it is necessary to consider that volume loss has occurred.

Particles can lose volume either to increases in density or loss of semivolatiles after collection onto a substrate, especially in a vacuum. The latter is particularly relevant for organic coated particles. Water is an important moderately volatile component of the deliquesced seed systems. While inorganic particles might hold a small amount of water after incomplete dehydration, viscous organics can retain a much higher volume of water after drying. Mikhailov et al. observed an increase in the mobility diameter of organic particles that underwent relative humidity cycling. Levoglucosan particles were hydrated to 60% RH and then dried to \sim 15% RH, similar to the humidifying and drying conditions for the experiments presented here. Residual water remained trapped in the semisolid structure upon drying on the time scale of seconds, or at least long enough to augment the measured D_m by 4%. The reported increase in particle D_m is attributed to the kinetically limited release of water through the formation of a glassy or gel-like semisolid organic structure at low relative humidities.

Here, for wet-seeded samples, deliquesced inorganic seeds were coated with secondary organic material and then rapidly dried and measured for mobility diameter. Either the encapsulation of the deliquesced seed droplets or the transformation of the organic coating to a semisolid may hold additional water in the particle and elevate the D_m measured immediately after the diffusion dryer. After sample collection, the trapped water may have sufficient time to diffuse through the organic layer while stored in desiccant and before microscope analysis. Semivolatile

organic compounds can also lead to losses in volume for deliquesced samples. As with water, if the coated particles do not have enough time reach equilibrium within the diffusion dryer, semivolatiles may continue to diffuse out of the viscous organic coating after the median D_m is measured by SMPS. Organic components may also continue to participate in particle phase reactions creating lower volatility products. In either the case of water or volatile organic loss, the total volume of the particle could decrease in storage or in the vacuum of the TEM, leading to the negative percent changes in median diameter observed for some secondary organic particles with dry seeds and all such particles with wet seeds.

In low growth particle populations, the water content of the inorganic seed at the time of coating influenced the spreading behavior of the final particle after drying for α -pinene SOA but not for limonene SOA. A small but statistically significant difference between the averages of the negative percent changes in the α-pinene low growth on dry and wet seeds shown in Table 2 was determined through a t-test. The modest negative percent changes are visible in the histograms in Figure 2, where the TEM-derived D_{pa} distribution is slightly negatively offset from the SMPSderived D_m distribution, indicating smaller particle diameters after impaction. Greater negative percent differences for wet-seeded low growth particles over dry-seeded particles were observed, which may be a consequence of either of two mechanisms: a larger loss in volatile species, particularly retained water unique to the deliquesced seeds, or a decrease in the degree of spreading from the greater ammonium sulfate or organic density resulting from restructuring during hydration, again unique to the wet-seeded populations. If both volume loss and spreading occur, as has been observed in our previous experiments for α -pinene low growth particles, ³⁹ either a larger loss of volume or reduction in spreading (or both) would lead to negative percent changes of larger magnitude for wet-seeded particles. For limonene low growth samples, populations with effloresced seeds gave the widest range of percent changes in median diameter of all of the low growth populations, and the only low growth sample with a positive percent change. Despite this, the average percent changes in median diameter were not significantly different between wet- and dry-seeded populations.

The percent changes for high growth experiments are not so straightforward. Our previous results indicated that high growth coatings of α-pinene secondary organic material on effloresced ammonium sulfate seeds show large negative and positive changes in diameter after impaction.³⁹ For the α -pinene experiments presented here, the large percent differences are mostly negative in sign for high growth populations on effloresced seeds and entirely negative in sign for high growth populations on deliquesced seeds, although a t-test did not show a significant difference between the two types of samples. Again, examples of these large percent differences for high growth on both dry and wet seeds are observable in Figure 3 in the large negative offsets between the TEMand SMPS-measured size distributions showing smaller particle diameters after impaction. High growth samples grown with limonene secondary organic material also did not show a significant difference in average percent changes to median diameter between wet- and dry-seeded samples, and gave only large negative percent change values. The larger magnitudes of the percent change values for high growth particles are seen in Figure S5 where the median diameters for high growth samples are further away from the one-to-one line than the low growth samples in almost all cases. There were also no significant differences between the average percent changes for high growth α-pinene and limonene organic coatings on seeds with corresponding water content (i.e. wet to wet and dry to dry), indicating that high growth samples spread an equivalent amount after impaction regardless of the SOA precursor used in this work or seed particle water content.

4.2.2 Morphology analysis

Beyond changes in diameter, each particle in secondary organic growth populations was assessed for the number of visible phases and was assigned a homogeneous morphology for particles with one visible phase and a phase-separated morphology for particles with two. The percentage of particles in each population presenting either morphology is shown in Tables 2 and 3 and the averages of these values for each type of growth sample is presented in Table 4. Particles with an ambiguous number of phases were not included in this analysis but were usually a small proportion of a sample population unless otherwise indicated. It is possible for particles to phase separate upon drying, however, this is unlikely as α-pinene secondary organic material has an oxygen:carbon ratio (O:C ratio) of 0.3 which means it has an estimated separation relative humidity of or greater than 90%. 52,53 At this O:C ratio, organic particles with deliquesced seeds are most likely liquid-liquid phase separated under the relative humidity conditions used in these experiments and before drying. While phase separated morphology is expected, homogeneous particles are also observed in coated samples. This observation may be because the organic coatings were too thin or too patchy to observe consistently, the coatings had an electron transmissivity close to ammonium sulfate, or the particles were not in an equilibrium state when collected and observed. For every combination of SOA precursor and seed water content, the average percentage of a population showing either phase separated or homogeneous morphologies as shown in Table 4 were tested pairwise against each other for statistical significance. The statistically significant results are noted and discussed below.

Table 4. Average Percentage of Particles within Populations of Each Sample Type Presenting either Phase-Separated or Homogeneous Morphologies

α-Piner	ne SOA	Limone	ne SOA	
Phase Separated	Homogeneous	Phase Separated	Homogeneous	

Dwy Soods	Low Growth	58% ± 19%	33% ± 18%	54% ± 35%	45% ± 36%
Dry Seeds	High Growth	$63\% \pm 27\%$	$30\% \pm 26\%$	$81\% \pm 8\%$	$11\% \pm 12\%$
Wat Sanda	Low Growth	41% ± 50%	$22\% \pm 41\%$	51% ± 29%	$60\% \pm 35\%$
Wet Seeds	High Growth	74% ± 19%	$15\% \pm 20\%$	57% ± 26%	$41\% \pm 26\%$

In general, high growth samples had more phase separated particles than low growth samples for all SOA precursors and water content conditions. Low growth samples by definition had thinner organic coatings, so differentiating a secondary outer phase was likely more difficult as the annular shell thickness for many of these samples was only a few nanometers thick. It follows that the higher growth samples had a higher percentage of obviously phase separated particles due to thicker and more visible organic coatings. Also, limonene secondary organic growth samples revealed more homogeneous particles than α-pinene secondary organic growth samples for three of the four growth conditions. Limonene secondary organic material is more likely to form homogeneous particles than α-pinene secondary organic material because limonene is more efficient at forming Extremely Low Volatility Organic Compounds (ELVOCs) through ozonolysis than α-pinene by a factor of 1.56.⁵⁴ ELVOCs are highly oxidized, polar compounds, which tend to be hygroscopic in nature, and make up a significant portion of first generation products formed through terpene ozonolysis.^{54,55} Because limonene is more efficient at forming ELVOCs, and thus, produces secondary organic material containing polar and more water soluble secondary organic products, limonene secondary organic/inorganic mixed particles may be more likely to form one homogeneous phase than α -pinene-derived mixed particles. The tendency for limonene SOA to form homogeneous structures is presumably especially pertinent when the inorganic core exists as a deliquesced droplet as with wet-seeded samples. Such an assumption is supported by the statistical significance between the limonene wet and dry high growth results as

well as the α -pinene and limonene wet high growth results. For the former significant result, limonene SOA particles showed a homogeneous morphology more often on deliquesced seeds than effloresced seeds, and for the latter, high growth particles with deliquesced seeds were more likely to be homogeneous when coated with limonene secondary organic material than with α -pinene secondary organic material. Relatedly, with statistical significance, there were more phase separated limonene high growth particles with effloresced seeds than deliquesced seeds as the solid inorganic core was unavailable for efficient mixing in dry-seeded samples.

α-Pinene and limonene growth samples with deliquesced seeds also showed a new textured morphology that was not observed in effloresced seed samples. As seen in panel D of Figures 2-5, wet-seeded organic particles were occasionally textured or "wrinkled" in appearance and had a less circular perimeter. Figure S6 shows representative images of three categories of phase separated particles made of secondary organic growth on deliquesced seeds: a phase separated particle with a typical round shape, a less circular and textured particle with pronounced phase separation, and a substantially textured particle with the lowest circularity and ambiguous phase state. While most wet-seeded organic particles fell into the first and second categories and could be classified as either phase separated or homogeneous, a classification of this kind could not be made for the most textured particles in the final category. When a determination of this kind could not be made, the area of the particle was measured for median diameter calculations but the phase was considered "undefined" and not included in either percent phase separated or percent homogeneous columns in Tables 2 and 3. Samples with a very high prevalence of particles with homogeneous or undefined phase states are not analyzed for core diameters and shell thicknesses as the statistical significance of the few particles displaying phase character would be low. Such measurements for these samples are marked NA in Tables 2 and 3.

The textured morphology seen in organic coated particles with deliquesced seeds is proposed to be a result of loss of water in the final drying step just before collection. The wet seed at the time of coating within the flow tube is larger than the final diameter of the seed after it is dried for collection (Figure S3). For samples of wet particles, the initial seeds are size selected while dry and then increase in volume when deliquescing in the CGC. It is difficult to measure the diameter of humidified particles, as maintaining a relative humidity within the SMPS matched to the flow tube is challenging, although the growth of a particle as it takes up water in high RH environments can be modeled using E-AIM. For reference, a 40 nm effloresced particle is predicted to increase in diameter to a 51 nm deliquesced particle at 60% RH, which corresponds to a 107% increase in volume. Similarly, a 60 nm effloresced particle is predicted to increase in diameter to a 78 nm deliquesced particle corresponding to a 119% increase in volume. This increased volume should be lost in the final diffusion dryer before sampling.

The viscous organic outer layer of a core-shell particle wrinkles as the particle loses water, introducing texture to the surface of the particle visible using TEM. For reference, α-pinene secondary organic material has been shown to be a highly viscous semisolid with viscosities on the order of 10⁴ to 10⁷ Pa·s at moderate relative humidities (40% RH to 70% RH) and 10⁸ Pa·s under dry conditions (below ~30% RH) like those used in the flow tube for these experiments. ^{56–58} Despite the lower viscosity of limonene secondary organic material, ⁵⁹ limonene and α-pinene SOA samples showed this textured morphology at roughly the same rate where slightly less than half of all wet-seeded organic particles had surface texture. None of the dry-seeded particles had a textured morphology because the wrinkling process does not occur for organic particles with effloresced seeds which remain approximately the same diameter throughout the flow tube apparatus; no loss of volume is experienced for effloresced seeds and dry-seeded organic particles

as there is no water to lose. Rapid drying rates within the diffusion drier may induce the textured morphology observed here. Drying rates have been shown to influence the morphology of mixed organic/inorganic particles,⁶⁰ and morphologies for organic growth on deliquesced seeds after slower drying should be assessed in future studies.

5. Conclusions and Implications

In summary, the water content of the inorganic seed particles in the flow tube reactor at the time of coating influenced the final size, shape, phase state, and surface interactions of particles composed of ammonium sulfate seeds coated with α -pinene or limonene secondary organic material and assessed using SMPS and TEM. For seed particles alone, seed phase was shown to influence the interactions between the particles and a substrate after impaction. Deliquesced seed particles spread less than effloresced particles due to changes in density after restructuring and drying. For coated particles, the majority of particles with a low growth of organic material showed negative percent changes in diameter after impaction for both wet- and dry-seeded samples, but the differences in α-pinene wet-seeded low growth samples were slightly more negative than limonene. Coated particles with a high level of organic growth exhibited diameter percent differences of the greatest magnitudes with high growth on dry seeds giving large positive and negative changes in diameter and high growth on wet seeds showing only large negative changes. The spreading behavior of all high growth particles, for either of the SOA precursors and seed particles with either water content used in this study were found to be virtually equivalent. Microscope analysis revealed that samples generated under high growth conditions generally had more phase separated particles and that limonene SOA produced more particles with homogeneous particles than α-pinene SOA for three of the four growth conditions. Also, a new textured morphology was observed which was dependent on the seed particle water content. Organic coatings on deliquesced seeds wrinkled upon drying, giving these particles a textured morphology that was not observed for the coated particles with effloresced seeds.

Seed particle water content is important to understand when considering the chemical and physical properties of atmospheric aerosol particles. Our results have implications for both laboratory experiments and atmospheric aerosol particles. Laboratory studies examining seeded secondary organic material should be conscientious of relative humidity and its effect on the phase state of an inorganic seed particle. Also, the propensity of an organic/inorganic mixed system for forming either coatings or well-mixed structures upon SOA formation should be considered carefully, with the recognition that it is possible that both morphologies are formed simultaneously. Climate models informed by laboratory experiments should also be particular about SOA formation parameters for the same reasons. Because of their pervasiveness in the environment, atmospheric aerosol particles are able experience wide variation in local environmental conditions including temperature, pressure, and humidity during their lifetime, from arid desert environments to the humidified marine boundary layer. The low and high relative humidity conditions for inorganic seed particles as they are coated in secondary organic material are atmospherically relevant. The water content of inorganic seed particles as related to experimental relative humidity should be explored further in conjunction with typically studied secondary organic formation parameters such as oxidant identity or UV processing. 5,13

Acknowledgment

E.C.T. and M.A.F. gratefully acknowledge support from NSF AGS-1916758. D.N.H. and M.V.J. gratefully acknowledge support from NSF AGS-1916819. The authors would like to thank H. L. Busse for contributions to the data analysis discussion.

Supporting Information Available: Details and schematic of the flow tube reactor configurations, illustrated depictions of the expected morphologies of particles at each step of generation, graphical representations of the D_{pa} vs. D_{m} relationship, and a description of the textured morphology and associated circularities.

References

- (1) Kanakidou, M.; Seinfeld, J. H.; Pandis, S. N.; Barnes, I.; Dentener, F. J.; Facchini, M. C.; Van Dingenen, R.; Ervens, B.; Nenes, A.; Nielsen, C. J.; Swietlicki, E.; Putaud, J. P.; Balkanski, Y.; Fuzzi, S.; Horth, J.; Moortgat, G. K.; Winterhalter, R.; Myhre, C. E. L.; Tsigaridis, K.; Vignati, E.; Stephanou, E. G.; Wilson, J. Organic Aerosol and Global Climate Modelling: A Review. *Atmospheric Chemistry and Physics* **2005**, *5* (4), 1053–1123. https://doi.org/10.5194/acp-5-1053-2005.
- (2) Kroll, J. H.; Seinfeld, J. H. Chemistry of Secondary Organic Aerosol: Formation and Evolution of Low-Volatility Organics in the Atmosphere. *Atmospheric Environment* **2008**, 42 (16), 3593–3624. https://doi.org/10.1016/j.atmosenv.2008.01.003.
- (3) Rudich, Y.; Donahue, N. M.; Mentel, T. F. Aging of Organic Aerosol: Bridging the Gap Between Laboratory and Field Studies. *Annual Review of Physical Chemistry* **2007**, *58* (1), 321–352. https://doi.org/10.1146/annurev.physchem.58.032806.104432.
- (4) Iinuma, Y.; Böge, O.; Miao, Y.; Sierau, B.; Gnauk, T.; Herrmann, H. Laboratory Studies on Secondary Organic Aerosol Formation from Terpenes. *Faraday Discussions* **2005**, *130* (0), 279–294. https://doi.org/10.1039/B502160J.
- (5) Rudich, Y. Laboratory Perspectives on the Chemical Transformations of Organic Matter in Atmospheric Particles. *Chem. Rev.* **2003**, *103* (12), 5097–5124. https://doi.org/10.1021/cr020508f.
- (6) Pye, H. O. T.; Chan, A. W. H.; Barkley, M. P.; Seinfeld, J. H. Global Modeling of Organic Aerosol: The Importance of Reactive Nitrogen (NO_x and NO₃). *Atmospheric Chemistry and Physics* **2010**, *10* (22), 11261–11276. https://doi.org/10.5194/acp-10-11261-2010.
- (7) Guenther, A.; Hewitt, C. N.; Erickson, D.; Fall, R.; Geron, C.; Graedel, T.; Harley, P.; Klinger, L.; Lerdau, M.; Mckay, W. A.; Pierce, T.; Scholes, B.; Steinbrecher, R.; Tallamraju, R.; Taylor, J.; Zimmerman, P. A Global Model of Natural Volatile Organic Compound Emissions. *Journal of Geophysical Research: Atmospheres* 1995, 100 (D5), 8873–8892. https://doi.org/10.1029/94JD02950.
- (8) Sindelarova, K.; Granier, C.; Bouarar, I.; Guenther, A.; Tilmes, S.; Stavrakou, T.; Müller, J.-F.; Kuhn, U.; Stefani, P.; Knorr, W. Global Data Set of Biogenic VOC Emissions Calculated by the MEGAN Model over the Last 30 Years. *Atmospheric Chemistry and Physics* **2014**, *14* (17), 9317–9341. https://doi.org/10.5194/acp-14-9317-2014.
- (9) Wainman, T.; Zhang, J.; Weschler, C. J.; Lioy, P. J. Ozone and Limonene in Indoor Air: A Source of Submicron Particle Exposure. *Environmental Health Perspectives* **2000**, *108* (12), 1139–1145. https://doi.org/10.1289/ehp.001081139.
- (10) Jokinen, T.; Berndt, T.; Makkonen, R.; Kerminen, V.-M.; Junninen, H.; Paasonen, P.; Stratmann, F.; Herrmann, H.; Guenther, A. B.; Worsnop, D. R.; Kulmala, M.; Ehn, M.; Sipilä, M. Production of Extremely Low Volatile Organic Compounds from Biogenic Emissions: Measured Yields and Atmospheric Implications. *Proceedings of the National Academy of Sciences* **2015**, *112* (23), 7123–7128. https://doi.org/10.1073/pnas.1423977112.

- (11) Rösch, C.; Wissenbach, D. K.; Franck, U.; Wendisch, M.; Schlink, U. Degradation of Indoor Limonene by Outdoor Ozone: A Cascade of Secondary Organic Aerosols. *Environmental Pollution* **2017**, *226*, 463–472. https://doi.org/10.1016/j.envpol.2017.04.030.
- (12) Hallquist, M.; Wenger, J. C.; Baltensperger, U.; Rudich, Y.; Simpson, D.; Claeys, M.; Dommen, J.; Donahue, N. M.; George, C.; Goldstein, A. H.; Hamilton, J. F.; Herrmann, H.; Hoffmann, T.; Iinuma, Y.; Jang, M.; Jenkin, M. E.; Jimenez, J. L.; Kiendler-Scharr, A.; Maenhaut, W.; McFiggans, G.; Mentel, T. F.; Monod, A.; Prévôt, A. S. H.; Seinfeld, J. H.; Surratt, J. D.; Szmigielski, R.; Wildt, J. The Formation, Properties and Impact of Secondary Organic Aerosol: Current and Emerging Issues. *Atmos. Chem. Phys.* **2009**, *9* (14), 5155–5236. https://doi.org/10.5194/acp-9-5155-2009.
- (13) Srivastava, D.; Vu, T. V.; Tong, S.; Shi, Z.; Harrison, R. M. Formation of Secondary Organic Aerosols from Anthropogenic Precursors in Laboratory Studies. *npj Clim Atmos Sci* **2022**, *5* (1), 1–30. https://doi.org/10.1038/s41612-022-00238-6.
- (14) Faust, J. A.; Wong, J. P. S.; Lee, A. K. Y.; Abbatt, J. P. D. Role of Aerosol Liquid Water in Secondary Organic Aerosol Formation from Volatile Organic Compounds. *Environ. Sci. Technol.* **2017**, *51* (3), 1405–1413. https://doi.org/10.1021/acs.est.6b04700.
- (15) Tolocka, M. P.; Jang, M.; Ginter, J. M.; Cox, F. J.; Kamens, R. M.; Johnston, M. V. Formation of Oligomers in Secondary Organic Aerosol. *Environ. Sci. Technol.* **2004**, *38* (5), 1428–1434. https://doi.org/10.1021/es035030r.
- (16) Higgins, D. N.; Taylor, M. S.; Krasnomowitz, J. M.; Johnston, M. V. Growth Rate Dependence of Secondary Organic Aerosol on Seed Particle Size, Composition, and Phase. *ACS Earth Space Chem.* **2022**, *6* (9), 2158–2166. https://doi.org/10.1021/acsearthspacechem.2c00049.
- (17) Song, C.; Gyawali, M.; Zaveri, R. A.; Shilling, J. E.; Arnott, W. P. Light Absorption by Secondary Organic Aerosol from α-Pinene: Effects of Oxidants, Seed Aerosol Acidity, and Relative Humidity. *Journal of Geophysical Research: Atmospheres* **2013**, *118* (20), 11,741-11,749. https://doi.org/10.1002/jgrd.50767.
- (18) Nestorowicz, K.; Jaoui, M.; Rudzinski, K. J.; Lewandowski, M.; Kleindienst, T. E.; Spólnik, G.; Danikiewicz, W.; Szmigielski, R. Chemical Composition of Isoprene SOA under Acidic and Non-Acidic Conditions: Effect of Relative Humidity. *Atmospheric Chemistry and Physics* **2018**, *18* (24), 18101–18121. https://doi.org/10.5194/acp-18-18101-2018.
- (19) Zhang, X.; McVay, R. C.; Huang, D. D.; Dalleska, N. F.; Aumont, B.; Flagan, R. C.; Seinfeld, J. H. Formation and Evolution of Molecular Products in α-Pinene Secondary Organic Aerosol. *PNAS* **2015**, *112* (46), 14168–14173. https://doi.org/10.1073/pnas.1517742112.
- (20) Liu, T.; Huang, D. D.; Li, Z.; Liu, Q.; Chan, M.; Chan, C. K. Comparison of Secondary Organic Aerosol Formation from Toluene on Initially Wet and Dry Ammonium Sulfate Particles at Moderate Relative Humidity. *Atmospheric Chemistry and Physics* **2018**, *18* (8), 5677–5689. https://doi.org/10.5194/acp-18-5677-2018.
- (21) Zhang, H.; Surratt, J. D.; Lin, Y. H.; Bapat, J.; Kamens, R. M. Effect of Relative Humidity on SOA Formation from Isoprene/NO Photooxidation: Enhancement of 2-Methylglyceric Acid and Its Corresponding Oligoesters under Dry Conditions. *Atmospheric Chemistry and Physics* **2011**, *11* (13), 6411–6424. https://doi.org/10.5194/acp-11-6411-2011.

- (22) Huang, J.-H.; Zhang, F.; Shi, Y.-P.; Cai, J.-R.; Chuang, Y.-H.; Hu, W.-P.; Lee, Y.-Y.; Wang, C. C. Water Plays Multifunctional Roles in the Intervening Formation of Secondary Organic Aerosols in Ozonolysis of Limonene: A Valence Photoelectron Spectroscopy and Density Functional Theory Study. *J. Phys. Chem. Lett.* **2023**, *14* (15), 3765–3776. https://doi.org/10.1021/acs.jpclett.3c00560.
- (23) Freedman, M. A. Phase Separation in Organic Aerosol. *Chem. Soc. Rev.* **2017**, *46* (24), 7694–7705. https://doi.org/10.1039/C6CS00783J.
- (24) Cohen, L.; Quant, M. I.; Donaldson, D. J. Real-Time Measurements of pH Changes in Single, Acoustically Levitated Droplets Due to Atmospheric Multiphase Chemistry. *ACS Earth Space Chem.* **2020**, *4* (6), 854–861. https://doi.org/10.1021/acsearthspacechem.0c00041.
- (25) Li, W.; Teng, X.; Chen, X.; Liu, L.; Xu, L.; Zhang, J.; Wang, Y.; Zhang, Y.; Shi, Z. Organic Coating Reduces Hygroscopic Growth of Phase-Separated Aerosol Particles. *Environ. Sci. Technol.* **2021**, *55* (24), 16339–16346. https://doi.org/10.1021/acs.est.1c05901.
- (26) Anttila, T.; Kiendler-Scharr, A.; Tillmann, R.; Mentel, T. F. On the Reactive Uptake of Gaseous Compounds by Organic-Coated Aqueous Aerosols: Theoretical Analysis and Application to the Heterogeneous Hydrolysis of N2O5. *J. Phys. Chem. A* **2006**, *110* (35), 10435–10443. https://doi.org/10.1021/jp062403c.
- (27) Folkers, M.; Mentel, Th. F.; Wahner, A. Influence of an Organic Coating on the Reactivity of Aqueous Aerosols Probed by the Heterogeneous Hydrolysis of N2O5. *Geophysical Research Letters* **2003**, *30* (12). https://doi.org/10.1029/2003GL017168.
- (28) Koop, T.; Bookhold, J.; Shiraiwa, M.; Pöschl, U. Glass Transition and Phase State of Organic Compounds: Dependency on Molecular Properties and Implications for Secondary Organic Aerosols in the Atmosphere. *Phys. Chem. Chem. Phys.* **2011**, *13* (43), 19238–19255. https://doi.org/10.1039/C1CP22617G.
- (29) Kuwata, M.; Martin, S. T. Phase of Atmospheric Secondary Organic Material Affects Its Reactivity. *Proceedings of the National Academy of Sciences* **2012**, *109* (43), 17354–17359. https://doi.org/10.1073/pnas.1209071109.
- (30) Veghte, D. P.; Altaf, M. B.; Haines, J. D.; Freedman, M. A. Optical Properties of Non-Absorbing Mineral Dust Components and Mixtures. *Aerosol Sci. Technol.* **2016**, *50* (11), 1239–1252. https://doi.org/10.1080/02786826.2016.1225153.
- (31) Freedman, M. A.; Hasenkopf, C. A.; Beaver, M. R.; Tolbert, M. A. Optical Properties of Internally Mixed Aerosol Particles Composed of Dicarboxylic Acids and Ammonium Sulfate. *J. Phys. Chem. A* **2009**, *113* (48), 13584–13592. https://doi.org/10.1021/jp906240y.
- (32) Zhang, Q.; Thompson, J. E. Effect of Particle Mixing Morphology on Aerosol Scattering and Absorption: A Discrete Dipole Modeling Study. *GeoResJ* **2014**, *3*–*4*, 9–18. https://doi.org/10.1016/j.grj.2014.07.001.
- (33) Jacobson, M. Z. Strong Radiative Heating Due to the Mixing State of Black Carbon in Atmospheric Aerosols. *Nature* **2001**, *409* (6821), 695–697. https://doi.org/10.1038/35055518.
- (34) Ovadnevaite, J.; Zuend, A.; Laaksonen, A.; Sanchez, K. J.; Roberts, G.; Ceburnis, D.; Decesari, S.; Rinaldi, M.; Hodas, N.; Facchini, M. C.; Seinfeld, J. H.; O' Dowd, C. Surface Tension Prevails over Solute Effect in Organic-Influenced Cloud Droplet Activation. *Nature* **2017**, *546* (7660), 637–641. https://doi.org/10.1038/nature22806.
- (35) Tillmann, R.; Hallquist, M.; Jonsson, Å. M.; Kiendler-Scharr, A.; Saathoff, H.; Iinuma, Y.; Mentel, T. F. Influence of Relative Humidity and Temperature on the Production of

- Pinonaldehyde and OH Radicals from the Ozonolysis of α-Pinene. *Atmospheric Chemistry and Physics* **2010**, *10* (15), 7057–7072. https://doi.org/10.5194/acp-10-7057-2010.
- (36) Qin, Y.; Ye, J.; Ohno, P.; Zhai, J.; Han, Y.; Liu, P.; Wang, J.; Zaveri, R. A.; Martin, S. T. Humidity Dependence of the Condensational Growth of α-Pinene Secondary Organic Aerosol Particles. *Environ. Sci. Technol.* **2021**, *55* (21), 14360–14369. https://doi.org/10.1021/acs.est.1c01738.
- (37) Riemer, N.; Ault, A. P.; West, M.; Craig, R. L.; Curtis, J. H. Aerosol Mixing State: Measurements, Modeling, and Impacts. *Reviews of Geophysics* **2019**, *57* (2), 187–249. https://doi.org/10.1029/2018RG000615.
- (38) Ott, E.-J. E.; Kucinski, T. M.; Dawson, J. N.; Freedman, M. A. Use of Transmission Electron Microscopy for Analysis of Aerosol Particles and Strategies for Imaging Fragile Particles. *Anal. Chem.* **2021**, *93* (33), 11347–11356. https://doi.org/10.1021/acs.analchem.0c05225.
- (39) Tackman, E. C.; Higgins, D. N.; Kerecman, D. E.; Ott, E.-J. E.; Johnston, M. V.; Freedman, M. A. The Use of Transmission Electron Microscopy with Scanning Mobility Particle Size Spectrometry for an Enhanced Understanding of the Physical Characteristics of Aerosol Particles Generated with a Flow Tube Reactor. *Aerosol Science and Technology* **2023**, *57* (4), 279–295.
- (40) Seinfeld, J. H.; Pandis, S. N. *Atmospheric Chemistry and Physics: From Air Pollution to Climate Change*, 3 edition.; Wiley: Hoboken, New Jersey, 2016.
- (41) Laskina, O.; Morris, H. S.; Grandquist, J. R.; Estillore, A. D.; Stone, E. A.; Grassian, V. H.; Tivanski, A. V. Substrate-Deposited Sea Spray Aerosol Particles: Influence of Analytical Method, Substrate, and Storage Conditions on Particle Size, Phase, and Morphology. *Environ. Sci. Technol.* **2015**, *49* (22), 13447–13453. https://doi.org/10.1021/acs.est.5b02732.
- (42) Lee, H. D.; Kaluarachchi, C. P.; Hasenecz, E. S.; Zhu, J. Z.; Popa, E.; Stone, E. A.; Tivanski, A. V. Effect of Dry or Wet Substrate Deposition on the Organic Volume Fraction of Core–Shell Aerosol Particles. *Atmospheric Measurement Techniques* **2019**, *12* (3), 2033–2042. https://doi.org/10.5194/amt-12-2033-2019.
- (43) Beaver, M. R.; Garland, R. M.; Hasenkopf, C. A.; Baynard, T.; Ravishankara, A. R.; Tolbert, M. A. A Laboratory Investigation of the Relative Humidity Dependence of Light Extinction by Organic Compounds from Lignin Combustion. *Environ. Res. Lett.* **2008**, *3* (4), 045003. https://doi.org/10.1088/1748-9326/3/4/045003.
- (44) Hsiao, T.-C.; Young, L.-H.; Tai, Y.-C.; Chen, K.-C. Aqueous Film Formation on Irregularly Shaped Inorganic Nanoparticles before Deliquescence, as Revealed by a Hygroscopic Differential Mobility Analyzer–Aerosol Particle Mass System. *Aerosol Science and Technology* **2016**, *50* (6), 568–577. https://doi.org/10.1080/02786826.2016.1168512.
- (45) Mikhailov, E.; Vlasenko, S.; Martin, S. T.; Koop, T.; Pöschl, U. Amorphous and Crystalline Aerosol Particles Interacting with Water Vapor: Conceptual Framework and Experimental Evidence for Restructuring, Phase Transitions and Kinetic Limitations. *Atmospheric Chemistry and Physics* **2009**, *9* (24), 9491–9522. https://doi.org/10.5194/acp-9-9491-2009.
- (46) Biskos, G.; Paulsen, D.; Russell, L. M.; Buseck, P. R.; Martin, S. T. Prompt Deliquescence and Efflorescence of Aerosol Nanoparticles. *Atmospheric Chemistry and Physics* **2006**, *6* (12), 4633–4642. https://doi.org/10.5194/acp-6-4633-2006.

- (47) Köllensperger, G.; Friedbacher, G.; Kotzick, R.; Niessner, R.; Grasserbauer, M. In-Situ Atomic Force Microscopy Investigation of Aerosols Exposed to Different Humidities. *Fresenius J Anal Chem* **1999**, *364* (4), 296–304. https://doi.org/10.1007/s002160051340.
- (48) Krämer, L.; Pöschl, U.; Niessner, R. Microstructural Rearrangement of Sodium Chloride Condensation Aerosol Particles on Interaction with Water Vapor. *Journal of Aerosol Science* **2000**, *31* (6), 673–685. https://doi.org/10.1016/S0021-8502(99)00551-0.
- (49) Ramesh, K. T. Nanomaterials: Mechanics and Mechanisms; Springer: New York, 2009.
- (50) Ashby, M. F. *Materials Selection in Mechanical Design*, 5th edition.; Butterworth-Heinemann: Amsterdam; Cambridge, MA, 2017.
- (51) Carlton, C.; Ferreira, P. J. What Is Behind the Inverse Hall-Petch Behavior in Nanocrystalline Materials? *MRS Online Proceedings Library (OPL)* **2006**, *976*, 0976. https://doi.org/10.1557/PROC-976-0976-EE01-04.
- (52) You, Y.; Renbaum-Wolff, L.; Carreras-Sospedra, M.; Hanna, S. J.; Hiranuma, N.; Kamal, S.; Smith, M. L.; Zhang, X.; Weber, R. J.; Shilling, J. E.; Dabdub, D.; Martin, S. T.; Bertram, A. K. Images Reveal That Atmospheric Particles Can Undergo Liquid–Liquid Phase Separations. *PNAS* **2012**, *109* (33), 13188–13193. https://doi.org/10.1073/pnas.1206414109.
- (53) Bertram, A. K.; Martin, S. T.; Hanna, S. J.; Smith, M. L.; Bodsworth, A.; Chen, Q.; Kuwata, M.; Liu, A.; You, Y.; Zorn, S. R. Predicting the Relative Humidities of Liquid-Liquid Phase Separation, Efflorescence, and Deliquescence of Mixed Particles of Ammonium Sulfate, Organic Material, and Water Using the Organic-to-Sulfate Mass Ratio of the Particle and the Oxygen-to-Carbon Elemental Ratio of the Organic Component. *Atmospheric Chemistry and Physics* **2011**, *11* (21), 10995–11006. https://doi.org/10.5194/acp-11-10995-2011.
- (54) Jokinen, T.; Berndt, T.; Makkonen, R.; Kerminen, V. M.; Junninen, H.; Paasonen, P.; Stratmann, F.; Herrmann, H.; Guenther, A. B.; Worsnop, D. R.; Kulmala, M.; Ehn, M.; Sipilä, M. Production of Extremely Low Volatile Organic Compounds from Biogenic Emissions: Measured Yields and Atmospheric Implications. *Proceedings of the National Academy of Sciences of the United States of America* **2015**, *112* (23), 7123–7128. https://doi.org/10.1073/pnas.1423977112.
- (55) Varutbangkul, V.; Brechtel, F. J.; Bahreini, R.; Ng, N. L.; Keywood, M. D.; Kroll, J. H.; Flagan, R. C.; Seinfeld, J. H.; Lee, A.; Goldstein, A. H. Hygroscopicity of Secondary Organic Aerosols Formed by Oxidation of Cycloalkenes, Monoterpenes, Sesquiterpenes, and Related Compounds. *Atmospheric Chemistry and Physics* **2006**, *6* (9), 2367–2388. https://doi.org/10.5194/acp-6-2367-2006.
- (56) Renbaum-Wolff, L.; Grayson, J. W.; Bateman, A. P.; Kuwata, M.; Sellier, M.; Murray, B. J.; Shilling, J. E.; Martin, S. T.; Bertram, A. K. Viscosity of α-Pinene Secondary Organic Material and Implications for Particle Growth and Reactivity. *Proceedings of the National Academy of Sciences* **2013**, *110* (20), 8014–8019. https://doi.org/10.1073/pnas.1219548110.
- (57) Reid, J. P.; Bertram, A. K.; Topping, D. O.; Laskin, A.; Martin, S. T.; Petters, M. D.; Pope, F. D.; Rovelli, G. The Viscosity of Atmospherically Relevant Organic Particles. *Nat Commun* **2018**, *9* (1), 956. https://doi.org/10.1038/s41467-018-03027-z.
- (58) Abramson, E.; Imre, D.; Beránek, J.; Wilson, J.; Zelenyuk, A. Experimental Determination of Chemical Diffusion within Secondary Organic Aerosol Particles. *Phys. Chem. Chem. Phys.* **2013**, *15* (8), 2983–2991. https://doi.org/10.1039/C2CP44013J.
- (59) Clará, R. A.; Marigliano, A. C. G.; Sólimo, H. N. Density, Viscosity, and Refractive Index in the Range (283.15 to 353.15) K and Vapor Pressure of α-Pinene, d-Limonene, (±)-

- Linalool, and Citral Over the Pressure Range 1.0 KPa Atmospheric Pressure. *J. Chem. Eng. Data* **2009**, *54* (3), 1087–1090. https://doi.org/10.1021/je8007414.
- (60) Altaf, M. B.; Freedman, M. A. Effect of Drying Rate on Aerosol Particle Morphology. *J. Phys. Chem. Lett.* **2017**, *8* (15), 3613–3618. https://doi.org/10.1021/acs.jpclett.7b01327.

TOC Figure

